Assessing dependence between soil ecosystem services as a function of weather and soil: Application of vine copula modeling

Tristan Senga Kiessé, Blandine Lemercier, Michael S. Corson, Yosra Ellili-Bargaoui, Jihad Afassi, Christian Walter

Assessing dependence between soil ecosystem services as a function of weather and soil: application of vine copula modeling

Tristan Senga Kiessé[1,*], Blandine Lemercier[1], Michael S. Corson[1], Yosra Ellili-Bargaoui[2], Jihad Afassi[1], Christian Walter[1]

[1]INRAE, Institut Agro, SAS, F-35000 Rennes, France

[2]Interact, UniLaSalle, F-60000 Beauvais, France

[*]*Corresponding author: tristan.senga-kiesse@inrae.fr* ORCID iD: 0000-0003-2710-5825

Abstract

Soils are natural ecosystems that provide ecosystem services, whose provision depends on multiple soil properties, climate conditions and human management. Dependence among soil ecosystem services (SESs) must therefore be considered to reliably assess risks of improving SES, as a function of weather conditions or soil properties. The present study described dependence among regulating and provisioning SESs predicted by a biophysical soil and crop model, based on a dataset of soils in France. We applied vine copula modeling as a statistical method that can model joint distribution functions of three SESs and enabled us to estimate probabilities of exceeding a level of one SES as a function of another SES. Trade-offs may need to be made between them to manage soil and water resources and achieve a given yield. By highlighting the degree of dependence among multiple SESs, copula models thus provide information that may improve understanding or management of ESs.

Keywords: dependence; soil ecosystem services; soil properties; weather conditions

Highlights

- Copulas modeled variable dependence between soil ecosystem services (SESs)
- Vine copula models analyzed multiple dependence by using pair-decomposition of SESs
- One SES could affect two other SESs separately, but not the dependence between them

1. Introduction

Soils are the focus of many studies since their multifunctional role is crucial as the central interface among the lithosphere, biosphere, hydrosphere and atmosphere (Dominati et al., 2014). Soils contribute to human welfare through the ecosystem services (ESs) that they provide

(Ellili-Bargaoui et al., 2021). Soil ESs (SESs) can be assessed using multiple indicators obtained by modeling biophysical processes and measuring multiple soil properties. For instance, maximum rooting depth and soil available water capacity are the indicators frequently used for ESs such as groundwater storage, plant biomass provision and water-quality regulation. Because ESs depend on the same biophysical processes and soil properties, many studies focus on dependence among ES to help develop policy strategies and make decisions about natural-resource management (Nelson et al., 2009). Describing dependence among ES highlights positive or negative correlations in which increasing one ES increases or decreases another one (i.e., a synergy or trade-off, respectively) (Lee and Lautenbach, 2016). Thus, there is practical interest in approaches that can investigate the distribution of ES of interest given the values of other ES, as a function of the environmental context (e.g., weather conditions, soil properties).

A variety of methods have been used to analyze relationships among ESs, such as regression models (e.g., generalized linear, additive), statistical tests of categorical variables (e.g., chi-square), principal component analysis (PCA) of quantitative variables and pairwise correlation coefficients, which is one of the most popular quantitative methods (Mouchet et al., 2014). PCA can help highlight contrasting relationships among SES and identify groups of soil sites as a function of given soil characteristics. Structural equation modeling, which is based on regression models that relate measured variables to "latent" (i.e., unmeasured) variables, can also help understand causal relationships between ES and explanatory variables (Grace, 2006; Leong et al., 2020). Relationships among ESs have been visualized using radial diagrams (Calzolari et al., 2016) and bagplots (Ellili-Bargaoui et al., 2021), and the latter have been used to map ESs in order to manage the ESs later (Egoh et al., 2008). In addition, optimal trade-offs between two SESs can be studied by plotting a curve (the "production possibility frontier" (Wu et al., 2021)) based on estimated responses of SESs to management practices in a variety of scenarios (see also Joly et al. (2021)). However, these approaches are generally limited by assumptions about input variables (e.g., independence), underlying data (e.g., normal distribution) or the shape (e.g., linear) of relationships between input variables and output variables used in models.

Copula modeling is a statistical method useful for constructing joint distribution functions that describe dependence between random variables (Sklar, 1959; Joe, 1993). They do not require making any assumptions about variables (e.g., that they follow a normal distribution) (Ching et al., 2014), unlike other statistical methods, and are particularly useful for detecting dependence when variables have simultaneously high or low values (i.e., "upper" or "lower tail-dependence", respectively) (Coles et al., 1999; Embrechts et al., 2002), which can occur during extreme events (e.g., droughts, market fluctuations). In particular, the class of "vine" copulas was developed to describe the dependence structure among multiple variables by building a model based on a variety of joint bivariate distribution functions (Czado and Nagler, 2022). Copula models have been applied to a wide range of topics, such as meteorological events and economics, for decades. For instance, copula models were used to describe how the dependence between rainfall and temperature influences agricultural production, to help study effects of climate change on crop yields (Cong and Brady, 2012). Likewise, copula models were recently used to describe the dependence structure among distributions of soil parameters that traditional multivariate normal distributions were unable to represent (Lü et al., 2020).

The aim of the present study was to model the pairwise dependence between a regulating SES (groundwater recharge or soil carbon (C) sequestration) and a provisioning SES (plant biomass provision). We then investigated the potential to increase the level of each of the regulating SESs. The pairwise dependence for the two regulating SESs was also analyzed as a function of a weather condition (i.e., effective rainfall (ER), equal to rainfall minus potential evapotranspiration) or a soil property (i.e., soil organic C (SOC) content), respectively. Rather than being measured in the field, the levels of the three SESs were predicted over 31 years using the STICS soil-crop model based on a dataset of 64 cultivated soils in northwestern France.

STICS is a one-dimensional mechanistic model that simulates crop development and soil processes that connect water, nitrogen (N) and C dynamics in the soil-plant-atmosphere continuum (Brisson et al., 2009). STICS has a daily time step and can simulate multiple consecutive years. Previous studies (e.g., Brisson et al. (2002); Schnebelen et al. (2004); Constantin et al. (2012); Constantin et al. (2015)) have evaluated the accuracy with which STICS predicted some of these outputs (including atypical values) for a variety of field and cover crops. A review of studies that used STICS to simulate 15 field crops at a total of 76 sites in France (Coucheney et al., 2015) considered that its accuracy was "very good" for whole-profile soil water content (mean relative root mean square error (rRMSE) = 10%) and "good" for plant fruit biomass at harvest (i.e., yield) (mean rRMSE = 33%). They concluded that STICS had sufficient accuracy and robustness for large-scale use under the soil and climate conditions in France. Similarly, predictions of changes in SOC content for seven long-term field experiments in Europe using the AMG model, on which STICS bases its simulation of SOC dynamics, were considered sufficiently accurate (rRMSE = 28%) (Levavasseur et al., 2020). We expected that by simulating the same crop rotation and weather for all 64 soil profiles, STICS would be able to predict relative differences among the profiles with sufficient accuracy for each of the three SESs studied.

2. Materials and Methods

2.1. Data

Soil dataset. The soil dataset contained data from 64 sites of cultivated land sampled in the department of Ille-et-Vilaine, in Brittany, northwestern France. Soil samples were collected at multiple depth intervals according to *GlobalSoilMap* specifications (Arrouays et al., 2014), and physico-chemical analyses of the samples were performed to measure properties such as SOC content (dry combustion) and pH (1:5 soil-to-water ratio, NF ISO 10390). See descriptive statistics of ER and SOC content (Table 1) and their scatterplots (Figure A1 in Supplementary material) of the soil profiles of the 64 sites from 1988-2018. See Ellili-Bargaoui et al. (2021) for more details.

Weather data. The Ille-et-Vilaine department has a temperate oceanic climate. Weather conditions were assumed to be the same for all 64 sites in the study area, an assumption supported by climate data from Météo France for 1981-2010 (Bretagne Environnement, 2020), which showed that, for nearly all sites, annual rainfall varied by no more than 200 mm (i.e., 700-900 mm), and mean annual temperature varied by no more than 1°C (i.e., 11-12°C). Weather data came from the weather station of Rennes-St Jacques, located near the center of the study area. Data such as daily rainfall (mm), mean air temperature (°C) and solar radiation (kW/m^2) were collected.

Crop-management data. Crop-management data reflected the main conventional crop rotation used by farmers in the study area: a 2-year rotation of grain maize (10 Apr-30 Oct), winter wheat (1 Nov-31 Jul) and a catch crop of white mustard (5 Sep-3 Mar). For grain maize and wheat, the soil was plowed to a depth of ca. 25 cm during the first five days of the period, and organic and inorganic fertilization was adjusted based on crop requirements, soil supplies and requirements of the European Union Nitrates Directive (EC, 1991) as specified in the French National Action Plan (OJFR, 2011).

2.2. Simulation modeling with STICS

Input parameters for STICS (version 9.0) came from the soil, weather and crop-management data. During the simulated study period, all soil parameters remained fixed except SOC, N and water contents, since they were influenced by crop development and weather conditions. STICS was used to simulate sequentially the three crops in the rotations at the 64 sites for 31 agricultural years (1988-2018) with the aid of a Java package developed to automate simulations. STICS provided more than 200 outputs, of which four daily outputs were selected to calculate indicators of the SESs: crop transpiration, crop yield, water drainage and SOC in humified organic matter. See Ellili-Bargaoui et al. (2021) for more details.

2.3. Soil ecosystem services

STICS outputs were used to estimate the level of the indicator of each SES (i.e., climate regulation, groundwater recharge, and plant biomass provision) for each calendar year simulated.

a. *Climate regulation* was estimated though C sequestration (CS), which represented the amount of organic C that the soil stored or released (positive or negative value, respectively). CS was quantified as the annual change in the stock of SOC in the topsoil (the top 30 cm):

$$CS_j = CStock_j - CStock_{j-1} \qquad \text{Equation 1}$$

where $CStock_j$ is the SOC stock in the topsoil in year j.

b. *Groundwater recharge* (GW) is the amount of water that percolates into the groundwater. GW was quantified as the annual sum of the water drained daily through the soil, which was assumed to reach the groundwater:

$$GW_j = \sum_{i=1}^{365} D_i \qquad \text{Equation 2}$$

where i is the day of year (1-365), and D_i is the amount of water drained daily from the soil (mm).

c. *Plant biomass provision* (YE) represents the soil's ability to produce plant biomass by photosynthesis. YE equals the annual yields of cash crops expressed as a unit of energy (GJ ha^{-1} $year^{-1}$):

$$YE_j = \frac{1}{n}\sum_{i=1}^{n} B_i \times k \qquad \text{Equation 3}$$

where B_i is the dry matter (t ha^{-1} year^{-1}) of harvested biomass, and k is the energy content of biomass: 14.905 and 13.984 GJt^{-1} fresh matter for maize and wheat grain, respectively (FAO, 2001).

After simulation modeling, the SES dataset contained 5952 variables for the SESs studied (3 SESs × 64 sites × 31 years of simulation). Sources of variation when predicting SESs corresponded to differences in weather conditions among years and to soil properties among sites, as the succession of field interventions was simulated on the same dates each year over the study period and for each soil profile. See descriptive statistics (Table 1) and scatterplots (Figure A1) for the three SESs of the soil profiles of the 64 sites from 1988-2018.

Table 1. Descriptive statistics of effective rainfall (ER, rainfall minus potential evapotranspiration) and soil organic carbon (SOC) content and predicted soil ecosystem services (groundwater recharge and plant biomass provision) of the 64 cultivated soil profiles (Ellili-Bargaoui et al., 2021), and for samples of the lowest (10th percentile) or highest (90th percentile) of ER and SOC contents

Variable	Data	Minimum	Mean	Maximum	Standard deviation
Effective rainfall (mm yr^{-1})	Entire dataset	-440	-256	-51	122
	Lowest ER	-440	-428	-417	8
	Highest ER	-97	-73	-51	15
SOC content (g/kg)	Entire dataset	10	20	45	7
	Lowest SOC contents	10	11	12	0.6
	Highest SOC contents	26	34	45	8
Plant biomass provision (GJ ha^{-1} yr^{-1})	Entire dataset	2	82	187	30
	Lowest ER	24	55	99	14
	Highest ER	39	87	179	28
	Lowest SOC contents	2	94	187	32
	Highest SOC contents	24	62	137	23
Groundwater recharge (mm yr^{-1})	Entire dataset	0	182	451	99
	Lowest ER	0	99	227	63
	Highest ER	76	288	441	74
	Lowest SOC contents	0	151	384	92
	Highest SOC contents	3	191	451	103
Climate regulation (kg C ha^{-1} yr^{-1})	Entire dataset	-1828	126	1279	344
	Lowest ER	-1454	199	1085	8
	Highest ER	-896	180	1279	15
	Lowest SOC contents	-602	189	950	263
	Highest SOC contents	-1828	-275	448	442

2.4. C-Vine Copula method

This section provides an overview of the copula method for modeling the dependence structure among three variables. Unlike other statistical methods, the vine copula method provides many functions to represent how three variables vary simultaneously by decomposing them into multiple bivariate functions. For more details, many articles review copulas comprehensively (Aas et al., 2009; Nagler, 2014; Nadarajah et al., 2018).

2.4.1. Vine copula decomposition

We consider continuous random variables X, Y and Z. Their marginal cumulative distribution functions (cdf) are denoted by F_X, F_Y and F_Z (i.e., probability of values falling below a threshold such that $F_X(x) = \Pr(X \leq x)$ (range: [0, 1])). Their probability density functions (pdf) are denoted by f_X, f_Y and f_Z (i.e., probability of falling within a particular range of values based on the shape of the distribution such that $\Pr(a \leq X \leq b) = \int_a^b f(x)dx$ (range: [0, 1])). Then, the triplet of variables (X, Y, Z) has a joint cdf $F(x, y, z) = \Pr(X \leq x, Y \leq y, Z \leq z)$ and a joint pdf denoted by f, which describes the simultaneous distribution of X, Y and Z. The cdfs F_X, F_Y, F_Z are unknown functions to estimate from data with the corresponding densities. We also denote the copula cdf as C and the copula pdf as c.

Given real variables X, Y and Z, a copula is a function that associates the triplet $\left(F_X(x),\ F_Y(y),\ F_Z(z)\right)$ in $[0, 1]^3$ of marginal cdfs to the joint cdf $F(x, y, z)$ in $[0, 1]$, as follows (Sklar, 1959):

$$C\left(F_X(x), F_Y(y),\ F_Z(z)\right) = F(x, y, z) \qquad \text{Equation 4}$$

By connecting F to F_X, F_Y and F_z, the copula function C describes the dependence among X, Y and Z, if it exists. "Canonical" vine (C-vine) copulas decompose the joint pdf f using various pair-copulas, such as

$$f(x, y, z) = \quad f_X(x) \cdot\ f_Y(y) \cdot\ f_Z(z) \qquad \text{Equation 5}$$

$$\cdot\, c_{xy}\left(F_X(x), F_Y(y)\right) \cdot c_{yz}\left(F_Y(y),\ F_Z(z)\right) \qquad (\mathrm{T}_1)$$

$$\cdot\, c_{xz|y}\left(F(x|y), F(z|y)\right), \qquad (\mathrm{T}_2)$$

where copulas c_{xy}, c_{yz} and $c_{xz|y}$ join X and Y, Y and Z, (X, Y) and (Y, Z), respectively, and $F(x|y)$ and $F(z|y)$ are conditional cdf (Aas et al., 2009). A C-vine copula represents the multivariate relationship f among X, Y and Z as a set of trees (T), which consist of nodes (i.e., variables) related by edges (i.e., bivariate copulas). Multiple decompositions can be developed depending on how the nodes are organized. Pair-copula decompositions are flexible tools that are useful for modeling dependence among variables of a high-dimensional model.

2.4.2. Bivariate parametric copulas

2.4.2.1. Examples

A variety of parametric copula classes (e.g., Archimedean, elliptical, extreme-value) have been developed to model various dependence structures between variables, such as positive or negative dependence (Nadarajah et al., 2018). Here, among the various copulas tested to fit the dependence structure between SESs, we illustrate bivariate parametric copulas used in the vine copula decomposition: the Archimedean copula "Frank" (Nagler, 2014) and the Gaussian copula. We first denote the copula by $C_\theta(u, v)$, with a parameter θ, $u = F_X(x)$ and $v = F_Y(y)$ in $[0, 1]$.

Example 1. The Frank copula ${C_\theta}^{Frank}$, with its real parameter $\theta \neq 0$, is defined by

$$ {C_\theta}^{Frank}(u, v) = \frac{1}{\ln\theta} \ln\left(1 + \frac{(\theta^u - 1)(\theta^{-v} - 1)}{\theta - 1}\right) \qquad \text{Equation 6} $$

The value of parameter θ provides information about the structure of copula ${C_\theta}^{Frank}$: $\theta > 1$ corresponds to negative dependence, θ around 1 corresponds to independence, and θ in]0, 1[corresponds to positive dependence.

Example 2. The Gaussian copula, with its parameter θ in [-1, 1], is defined by

$$ {C_\theta}^{Gauss}(u, v) = \frac{1}{2\pi\sqrt{1 - \theta^2}} \int_{-\infty}^{\phi^{-1}(u)} \int_{-\infty}^{\phi^{-1}(v)} e^{\left(\frac{x^2 - 2\theta xy + y^2}{2(1-\theta^2)}\right)} dxdy \qquad \text{Equation 7} $$

where ϕ^{-1} is the inverse of the univariate standard normal cdf. The value of parameter θ in [-1, 0[corresponds to negative dependence, θ around 0 corresponds to independence, and θ in]0, 1] corresponds to positive dependence.

2.4.2.2. Copula selection and goodness-of-fit tests

We considered independent realizations $(x_i, y_i), i = 1, \dots, n$, from the pair (X, Y) of continuous random variables with their marginal cdf F_X and F_Y. The selection procedure first consisted of fitting several copulas from the main copula classes. For each copula C_θ considered, an estimate $\hat{\theta}_n$ of parameter θ was first calculated using the method of maximum likelihood such that

$$\hat{\theta}_n = \underset{\theta}{\operatorname{argmax}} \sum_{i=1}^{n} \ln c_\theta(u_i, v_i)$$ Equation 8

where c_θ is the copula pdf and (u_i, v_i) are the pairs obtained by transforming realizations (x_i, y_i) to uniform margins on $[0, 1]^2$, which must be done before applying Equation 8. We then selected the copula that minimized the Akaike Information Criterion (AIC), given by

$$AIC_n = -2 \sum_{i=1}^{n} \ln \left(c_{\hat{\theta}_n}(u_i, v_i) \right) + 2p$$ Equation 9

where p is the dimension of parameter θ in the copula (= 1 for the Frank and Gaussian copulas).

Once one copula $C_{\hat{\theta}_n}$ with the estimate $\hat{\theta}_n$ of its parameter was selected, the scatterplot of pairs of observations was compared to $N = 1000$ random pairs simulated using the Monte Carlo (MC) method from copula $C_{\hat{\theta}_n}$. The MC method is well adapted for simulating relationships among multiple dependent variables (Li et al., 2013), such as copulas, thus extrapolating a relatively small sample to a much larger one and increasing the robustness of the results obtained. Simulating random pairs from selected copula required finding the estimates $\hat{F}_X$ and $\hat{F}_Y$ of cdf F_X and F_Y. All analyses were performed in R software (R Core Team, 2020) using packages that applied the copula method, such as *VineCopula* (Schepsmeier et al., 2015).

2.5. Application of the copula method

We used results of copula models to estimate the probability of exceeding a level of a regulating SES as a function of the provisioning SES, by considering given weather conditions or soil properties. The C-vine copula was first applied to model joint cdfs of the three SESs (GW, CS and YE) calculated from STICS predictions, and classes of bivariate copulas that joined pairs of SESs were identified. Using maximum likelihood estimation, we tested lognormal, gamma, Weibull and normal pdfs to fit marginal distributions of each SES based on the Kolmogorov-Smirnov test (Figures A2 and A3). Conditional probabilities of one regulating SES (GW or CS) exceeding a threshold given that the provisioning SES (YE) exceeded another threshold were calculated (Box 1, Supplementary material). To this end, thresholds of GW, CS and YE were defined according to the range in which each SES varied in the soil dataset. Thresholds y of YE were varied from 20-100 GJ ha^{-1} yr^{-1}, with a step of 20 GJ ha^{-1} yr^{-1}, to consider a range of YE when considering the lowest or highest ER among all sites. For reference, mean (2000-2020) yields of maize grain and soft winter wheat in the study area (8.52 and 7.31 t ha^{-1} of fresh matter, respectively) (Agreste, 2021) would provide a mean of 114.6 GJ ha^{-1} yr^{-1} over the 2-year rotation. Thresholds g of GW were varied from 0-250 and 75-500 mm yr^{-1}, with a step of 25 mm yr^{-1}, when considering the lowest or highest ER among all sites, respectively. Thresholds c of CS were varied from -600 to 1000 kg C ha^{-1} yr^{-1} when considering the lowest or highest ER among all sites, and from -1200 to 600 kg C ha^{-1} yr^{-1} or -600 to 600 kg C ha^{-1} yr^{-1} when considering the lowest or highest SOC contents among all sites, respectively (with a step of 100 kg C ha^{-1} yr^{-1} for both). We focused in particular on the CS threshold of 0, at which soils began to sequester SOC instead of releasing it.

Dependence among the three SESs was modeled for the lowest (10th percentile) or highest (90th percentile) of ER and for the lowest (10th percentile) or highest (90th percentile) SOC contents among all sites (Table 1). The percentiles of ER contained 199 values each (i.e. 10% of the total sample of 64 sites × 31 years = 1984). In comparison, the percentiles of SOC content contained 217 values each because the observed SOC content, used as the initial SOC content in the simulations, remained the same for each site for all 31 simulated years (i.e., the total sample contained 64 sets of 31 identical SOC contents; thus, no part of any set could be excluded from a percentile). Conditional probabilities were calculated from the N = 1000 points simulated from the selected copula using the MC method for the pairs of SESs considered (Equation A2).

3. Results

3.1. 10th and 90th percentiles

Because the same weather data were used for all 64 sites, estimates of ER for a given year varied little among sites, due to small differences in predicted potential evapotranspiration caused by differences in soil depth and predicted water-holding capacity. Thus, the 10th percentile of ER contained all 64 sites for the three driest years (i.e., 1989, 2005 and 2010) and 7 sites for the next driest year (i.e. 1990). The 90th percentile of ER contained all 64 sites for the three wettest years (i.e., 1998, 1999 and 2000) and 7 sites for the next wettest year (i.e., 2014). In comparison, because SOC content is site-specific, and the observed SOC content was used only to initialize the simulations, the 10th and 90th percentiles of SOC content each contained 7 sites for all 31 simulated years. The soils with the lowest SOC contents among all sites developed from recent marine alluvium (sandy to silty-loam deposits) or Aeolian loam. Both parent materials provide conditions for low SOC content: nearly neutral or high pH and great depth, fine texture and absence of coarse fragments, which allows for relatively intense and deep plowing that may have led to relatively low SOC content. In contrast, most of the soils with the highest SOC contents among all sites were in the Dol-de-Bretagne marsh and developed from alternating continental and marine alluvia, which have naturally high clay and SOC contents.

3.2. Dependence among GW, CS and YE as a function of effective rainfall

When fitting a C-vine copula to data of the three SESs studied, Frank copulas best fit the dependence structure between GW and YE and CS and YE (Figure 1), but with different estimated values $\hat{\theta}_n$ of the copula parameter for the lowest and highest ER. GW was negatively correlated with YE (Kendall correlation coefficients $\hat{\tau}_n < 0$) when considering the lowest or highest ER among all sites (Table 2) and the entire dataset (Figure A1). Conversely, CS was positively ($\hat{\tau}_n > 0$) and negatively ($\hat{\tau}_n < 0$) correlated with YE when considering the lowest or highest ER, respectively, compared to a positive correlation when considering the entire dataset. Differing orientations and shapes of contour plots illustrated the sign (positive or negative) and strength (high or low), respectively, of correlations between CS and YE as a function of ER (Figure 1).

No tail dependences were identified between each pair of SESs due to the lack of soil profiles that had simultaneously low or high values of GW or CS and YE (Figure 1). Conversely, copulas modeled soil profiles in which GW or CS was lower when YE was higher, and vice-versa. C-vine copulas also modeled an independence structure (i.e., a more circular contour) between the pairs (GW, YE) and (CS, YE) when considering either the lowest or highest ER (Figure 1). Thus, YE influenced GW and CS separately, but did not influence the dependence between GW and CS.

Table 2. Kendall correlation coefficients $\hat{\tau}_n$ between pairs of soil ecosystem services (SESs) (climate regulation (CS), groundwater recharge (GW), and plant biomass provision (YE)) and/or weather condition (effective rainfall (ER)) and soil property (organic carbon (SOC) content) of soil profiles associated with the lowest or highest ER and lowest or highest SOC contents among all sites. Bold values indicate significant correlations ($p < 0.05$).

	Lowest ER				Highest ER			
SES	CS	GW	YE	ER	CS	GW	YE	ER
CS	1.00	-0.03	**0.13**	**-0.30**	1.00	0.07	**-0.19**	**-0.31**
GW		1.00	**-0.37**	0.17		1.00	**-0.44**	0.05
YE			1.00	-0.06			1.00	0.19
	Lowest SOC content				Highest SOC content			
SES	CS	GW	YE	SOC	CS	GW	YE	SOC
CS	1.00	0.06	**-0.10**	**0.20**	1.00	**0.25**	-0.07	**-0.49**
GW		1.00	0.01	**0.08**		1.00	-0.05	**-0.14**
YE			1.00	**-0.22**			1.00	-0.08

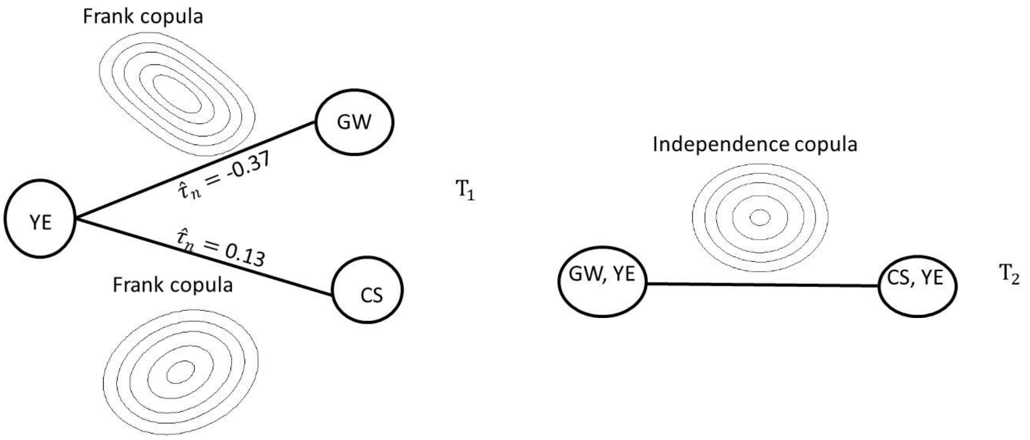

(a) Lowest ER

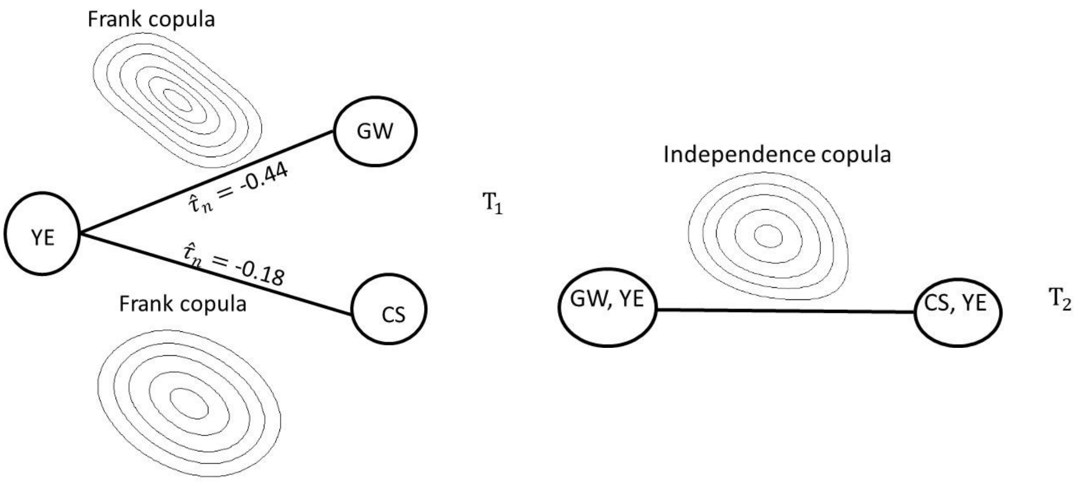

(b) Highest ER

Figure 1. Trees (T_1 and T_2) of canonical vine copulas and contours of bivariate copulas selected to model dependence among groundwater recharge (GW), carbon sequestration (CS) and plant biomass provision (YE) calculated from predictions of the STICS model for sites with the (a) lowest effective rainfall (ER) or (b) highest ER. $\hat{\boldsymbol{\tau}}_{\boldsymbol{n}}$ is the Kendall correlation coefficient.

3.2.1. Groundwater recharge as a function of plant biomass provision

The dependence between GW and YE modeled by Frank copulas was investigated first. The two scatterplots of 199 points calculated from STICS predictions for sites with the lowest or highest ER and of 1000 points extrapolated from the fitted copulas overlapped almost completely, which indicated that these copulas represented the predictions satisfactorily (Figure 2b, d).

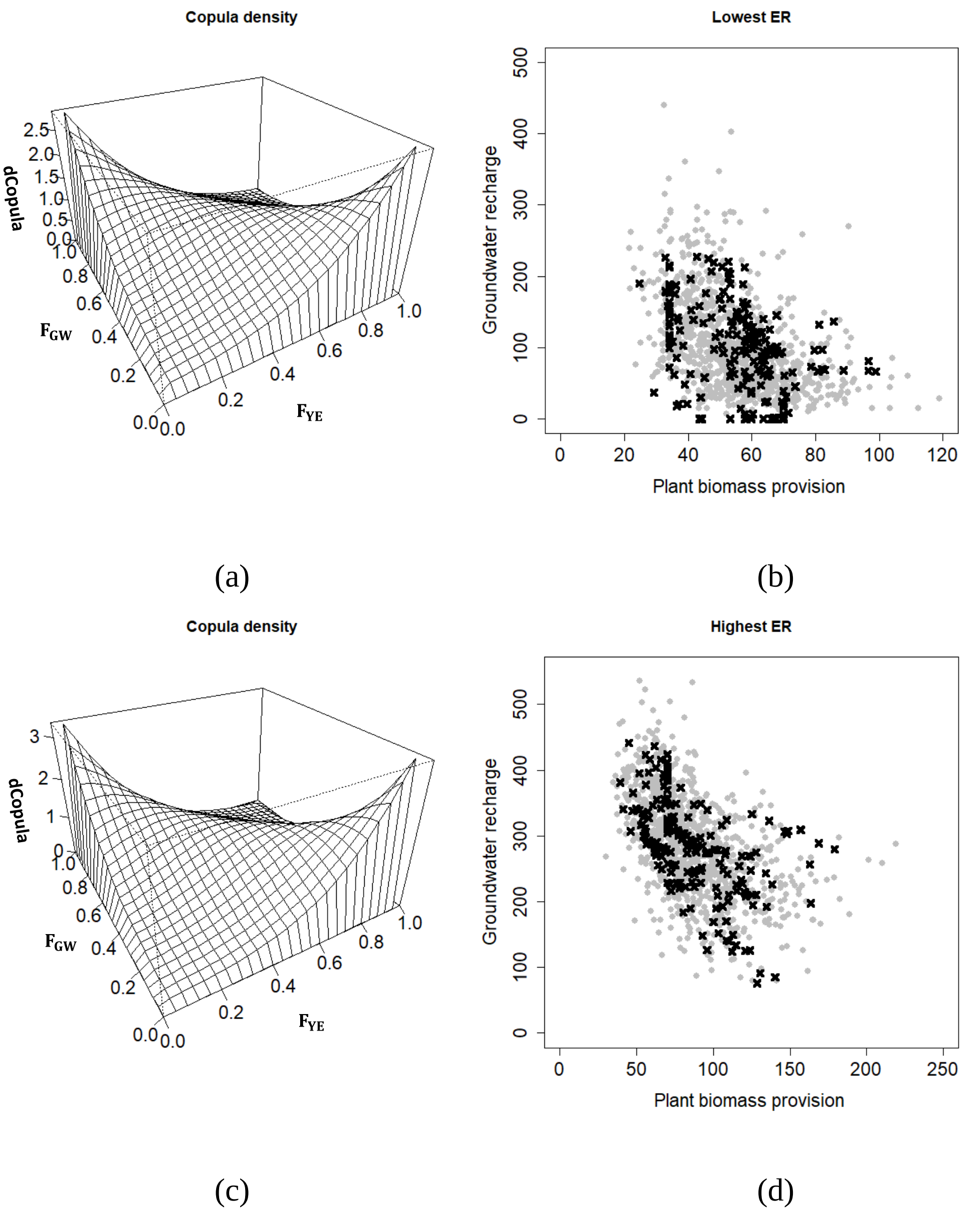

Figure 2. (a, c) Density functions of Frank copulas selected to model the dependence between univariate marginal cumulative distribution functions of groundwater recharge (GW, mm yr^{-1}) and plant biomass provision (YE, GJ ha^{-1} yr^{-1}) calculated from predictions of the STICS model for sites with the (a, b) lowest effective rainfall (ER) or (c, d) highest ER extrapolated from a random sample (gray circles) of N = 1000 from the fitted copula. Black crosses represent 199 points from STICS predictions.

Based on values extrapolated from the chosen copula, the probability of GW exceeding a given threshold logically decreased as this threshold increased from 0 to 250 mm yr^{-1} for the lowest ER or from 75 to 500 mm yr^{-1} for the highest ER, for a given threshold of YE (Figure 3, Tables A1 and A2). In addition, as the threshold of YE increased from 20 to 100 GJ ha^{-1} yr^{-1}, the probability of GW exceeding a given threshold decreased. For instance, as the threshold of YE increased from 20 to 60 GJ ha^{-1} yr^{-1}, the probability of exceeding 100 mm yr^{-1} for the lowest ER decreased from 0.42 to 0.16 and that of exceeding 300 mm yr^{-1} during the highest ER decreased from 0.43 to 0.24.

When varying thresholds of YE, the probability of exceeding a given threshold of GW varied more when considering the lowest ER than the highest ER. The threshold of YE had little influence on the probability of GW exceeding a minimum or maximum threshold, but it had a strong influence on the probability of GW exceeding intermediate thresholds. The variability in probability was particularly high for certain thresholds of GW for the lowest or highest ER. For instance, the probability of exceeding GW thresholds of 50 or 100 mm yr^{-1} for the lowest ER (the latter close to the mean for these ER (Table 1)) was 0.25-0.77 and 0-0.42, respectively, as the threshold of YE varied. Likewise, the probability of exceeding a GW threshold of 200 or 300 mm yr^{-1} during the highest ER (the latter close to the mean for these ER (Table 1)) was 0.78-0.89 and 0.17-0.43, respectively, as the threshold of YE varied.

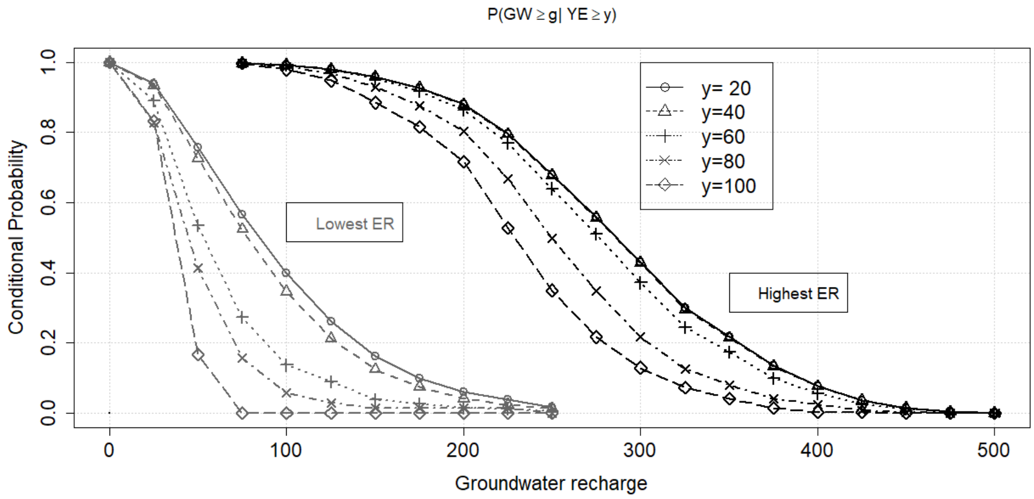

Figure 3. Conditional probabilities of groundwater recharge (GW) (mm yr^{-1}) exceeding given thresholds (“g”) as a function of plant biomass provision (YE, GJ ha^{-1} yr^{-1}) exceeding given thresholds (“y”) from extrapolation of STICS predictions for sites with the lowest effective rainfall (ER) (gray lines) or highest ER (black lines)

3.2.2. Carbon sequestration as a function of plant biomass provision

The conditional probability of CS exceeding a given threshold logically decreased as this threshold increased from -600 to 1000 kg C ha^{-1} yr^{-1} for the lowest and highest ER, for a given threshold of YE. As the threshold of YE increased from 20 to 100 GJ ha^{-1} yr^{-1}, the probability of CS exceeding a given threshold increased for the lowest ER (Figure 4a) but decreased for the highest ER (Figure 4b). In addition, for the same thresholds of CS and YE, the probability of CS exceeding a given threshold was generally higher for the lowest ER than for the highest ER. For instance, the probability of exceeding the CS threshold of 0 was 0.70-1.00 for the lowest ER and 0.50-0.70 for the highest ER.

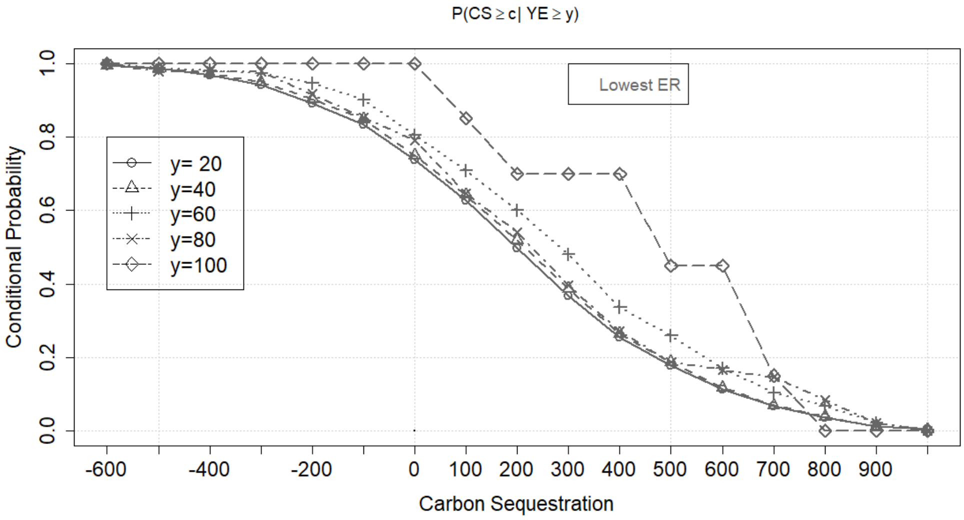

(a)

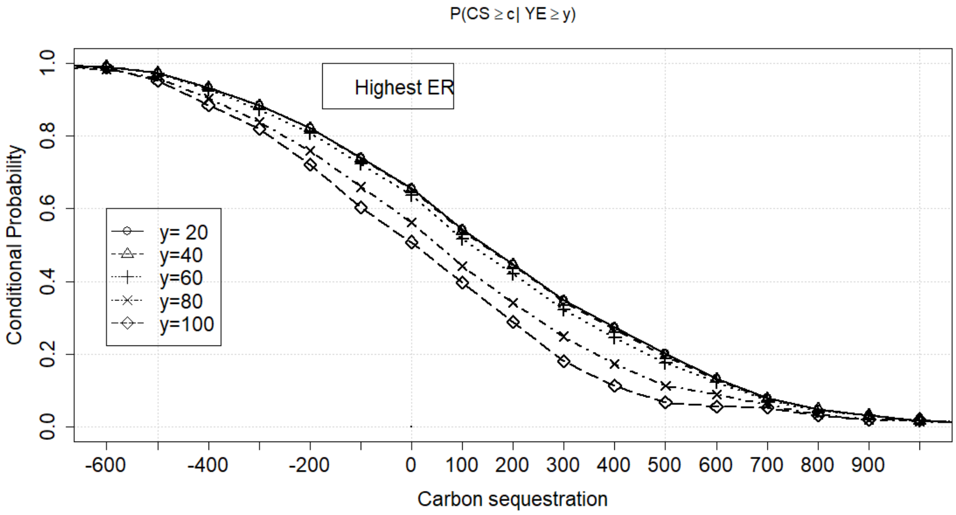

(b)

Figure 4. Conditional probabilities of carbon sequestration (CS) (kg C ha^{-1} yr^{-1}) exceeding given thresholds ("c") as a function of plant biomass provision (YE, GJ ha^{-1} yr^{-1}) exceeding given thresholds ("y") from extrapolation of STICS predictions for sites with the (a) lowest effective rainfall (ER) or (b) highest ER

3.3. Dependence among GW, CS and YE as a function of soil organic carbon content

When considering sites with the lowest SOC contents, the correlation between CS and YE was weak (-0.10) but significant (Table 1), and a Gaussian copula with $\hat{\theta}_n$ equal to -0.15 (i.e., negative dependence) best fit the dependence between them (Figure 5). The correlation between

CS and GW was also weak (0.06) but not significant, and an independence copula fit the relationship between these two SES. Likewise, an independence copula fit the relationship between (GW, CS) and (YE, CS), which indicated that CS did not influence the relationship between GW and YE. When considering sites with the highest SOC contents, the correlation between CS and GW was significant (0.25), and a Gaussian copula with $\hat{\theta}_n$ equal to 0.39 fit the dependence between them. An independence copula fit the relationship between CS and YE, as well as that between (GW, CS) and (YE, CS) (Figure 5).

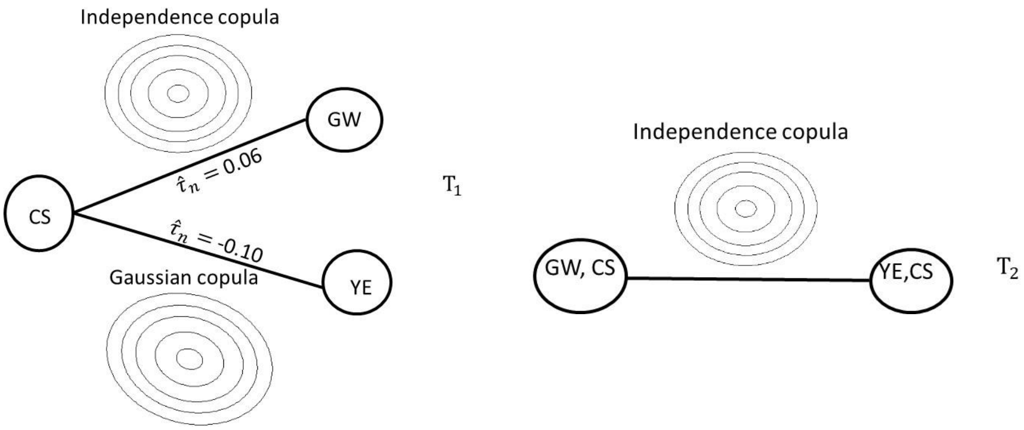

(a) Lowest SOC contents

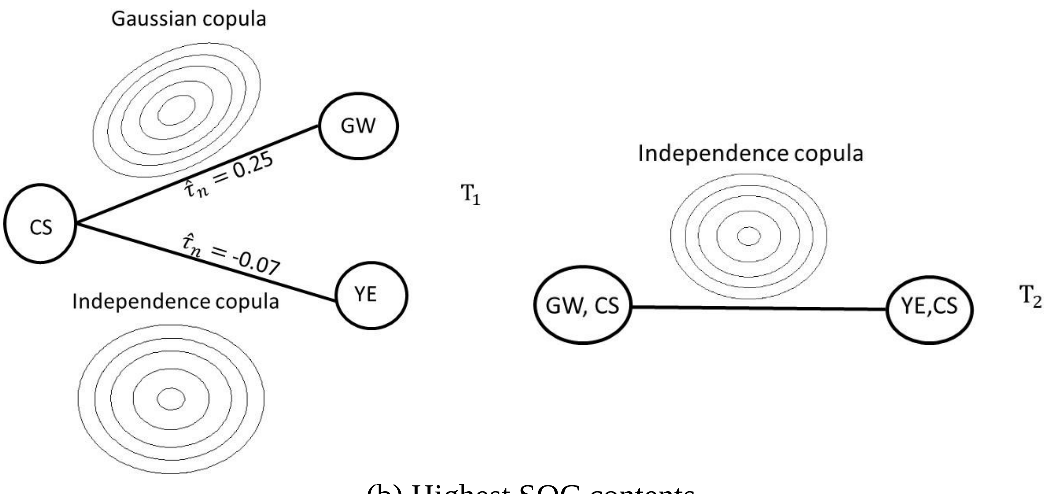

(b) Highest SOC contents

Figure 5. Trees (T_1 and T_2) of canonical vine copulas and contours of bivariate copulas selected to model the dependence among groundwater recharge (GW), carbon sequestration (CS) and plant biomass provision (YE) calculated from predictions of the STICS model for sites with the (a) lowest or (b) highest organic carbon (SOC) contents. $\boldsymbol{\hat{\tau}_n}$ is the Kendall correlation coefficient.

3.3.1. Carbon sequestration as a function of plant biomass provision

The modeled dependence between CS and YE was then investigated. The two scatterplots of 217 points calculated from STICS predictions for sites with the lowest or highest SOC contents and of 1000 points extrapolated from the chosen copulas overlapped almost completely (Figure A6). Like the dependence between GW and YE, the conditional probability of CS exceeding a given threshold logically decreased as this threshold increased from -600 to 600 kg C ha^{-1} yr^{-1} for the lowest SOC contents or from -1200 to 600 kg C ha^{-1} yr^{-1} for the highest SOC contents, for a given threshold of YE (Figure 6, Tables A3 and A4). The conditional probability of CS exceeding a given threshold was influenced slightly or not all by the YE threshold, which reflected the weak correlation or independence between CS and YE for the lowest or highest SOC contents, respectively. For instance, the probabilities of exceeding CS thresholds of 0 and 300 kg C ha^{-1} yr^{-1} for the lowest SOC contents were 0.71-0.75 and 0.28-0.33, respectively, as the threshold of YE varied. Likewise, the probabilities of exceeding the same two thresholds for the highest SOC contents were 0.21-0.27 and 0.07-0.09, respectively, as the threshold of YE varied. Thus, for the same thresholds of CS and YE, the conditional probability of CS exceeding a given threshold was higher for sites with the lowest SOC contents than for those with the highest SOC contents.

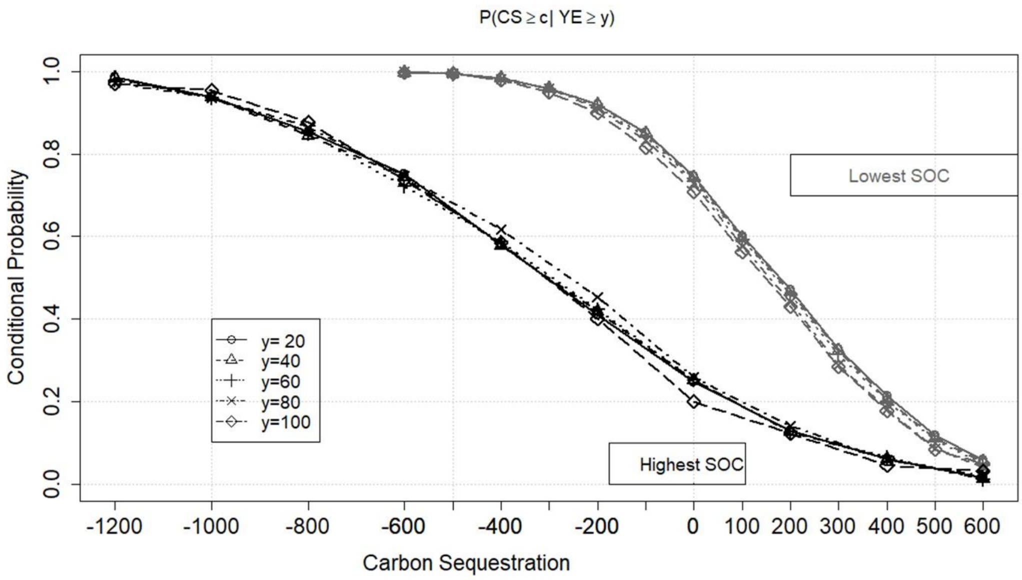

Figure 6. Conditional probabilities of carbon sequestration (CS) exceeding given thresholds (“c”) (kg C ha^{-1} yr^{-1}) as a function of plant biomass provision (YE, GJ ha^{-1} yr^{-1}) exceeding given thresholds (“y”) from extrapolation of STICS predictions for sites with the (a) lowest (gray lines) or (b) highest (black lines) soil organic carbon (SOC) contents.

4. Discussion

4.1. Probabilities of exceeding ecosystem service thresholds

4.1.1. Groundwater recharge as a function of plant biomass provision

Results of copula modeling helped analyze the potential to achieve certain target levels of regulating SESs (GW and CS) as a function of variations in a provisioning SES (YE), weather conditions and a soil property (i.e., SOC content). The dependence that we observed between YE and GW is well documented in the literature and can be explained by considering the soil water balance (Radcliffe and Simunek, 2012). Higher crop yields increase the flow of water to the atmosphere via transpiration, which decreases soil water content and the amount of water likely to drain below the root system. Thus, most studies that analyzed the relationship between YE and GW identified a significantly negative correlation between them (e.g., -0.71 in southern France (Demestihas et al., 2018), -0.86 for the mean annual data considered in the present study (Figure A5) (Ellili-Bargaoui et al., 2021)). Their magnitude, however, depends on annual weather conditions, as shown by applying the copula method. The relationship between YE and GW also depended on their ranges of variation, with lower conditional probabilities of exceeding a given level of GW during the wettest years (i.e., less variation) than the driest years (i.e., more variation) (Figure 3). Placing these conditional probabilities in a decision tree, GW was more likely to exceed thresholds close to its mean value (i.e., 100 and 250 mm yr^{-1} in the wettest and driest years, respectively (Table 1)) during the wettest years than the driest years, when considering YE exceeding thresholds of 40, 60 and 80 GJ ha^{-1} yr^{-1} (Figure 7). Thus, when GW becomes an issue for the supply of drinking water or preservation of aquatic environments, such as after a dry winter, certain management practices (e.g., decreasing fertilization) could be used as a mechanism to limit YE in order to ensure sufficient levels of GW. The decision tree based on copula models provides indications of the yield that could be targeted depending on the level of GW desired, and the associated conditional probability.

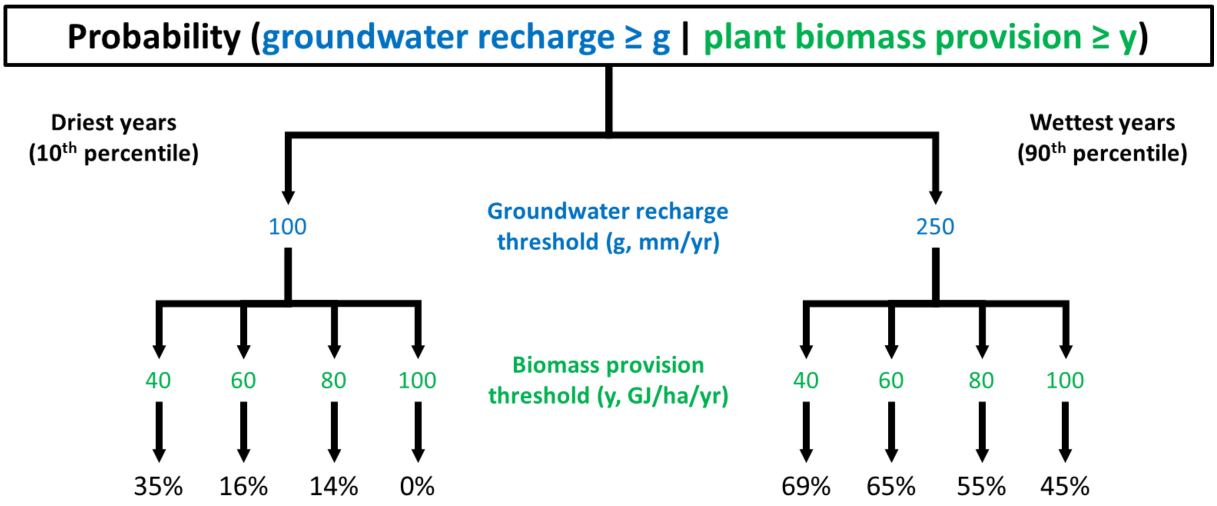

Figure 7. A decision tree of conditional probabilities of groundwater recharge (GW) exceeding a given threshold 'g' (mm yr^{-1}) as a function of plant biomass provision (YE) exceeding a given threshold 'y' (GJ ha^{-1} yr^{-1}) from extrapolation of STICS predictions for sites with the lowest or highest effective rainfall (i.e., driest or wettest years, respectively). For reference, mean yields of maize grain and wheat (8.52 and 7.31 t ha^{-1}, respectively) in the study area would provide a mean of 114.6 GJ ha^{-1} yr^{-1} over the 2-year rotation.

4.1.2. Carbon sequestration as a function of plant biomass provision

The dependence that we observed between yield YE and CS is more complex, since CS depends on the initial SOC and the type of crop considered, but also on management practices such as fertilization and the removal or incorporation crop residues (Lemke et al., 2010; Paustian, 2014). The predictions used in our study assumed that all crop residues were removed. The threshold of YE influenced the probability of CS exceeding a given threshold when ER varied (i.e., driest vs. wettest years) (Figure 4). The CS may have been higher during the driest years in part because dry conditions decrease mineralization of organic matter by microorganisms (Thapa et al., 2021). Mineralization may also explain why, as YE increased, CS increased during the driest years but decreased during the wettest years. Temperature was not considered as a variable in the copula models, but it also influences mineralization in the field and the STICS model. Conversely, the threshold of YE had almost no influence on the probability of CS exceeding a given threshold when the SOC content in the topsoil varied (i.e., lowest vs. highest) (Figure 6). In this context, modifying YE may or may not be used as a mechanism to increase the probability of CS exceeding a given threshold (Figure A4).

YE was weakly negatively correlated with SOC (-0.22) (Figure A1). A soil's capacity to sequester C (i.e., positive CS) depends on its physicochemical properties, especially clay content (Churchman et al., 2020), and negative CS (i.e., loss of SOC) is considered a "disservice" (Olson et al., 2017). The probabilities that CS exceeded high thresholds (e.g., 300 kg C ha^{-1} yr^{-1}) were low, since soils tend towards saturation in SOC content. Consequently, soils were more likely to sequester C when considering the lowest SOC contents (0.71-0.75) than the highest SOC contents (0.21-0.27), regardless of the threshold of YE (Figure 8).

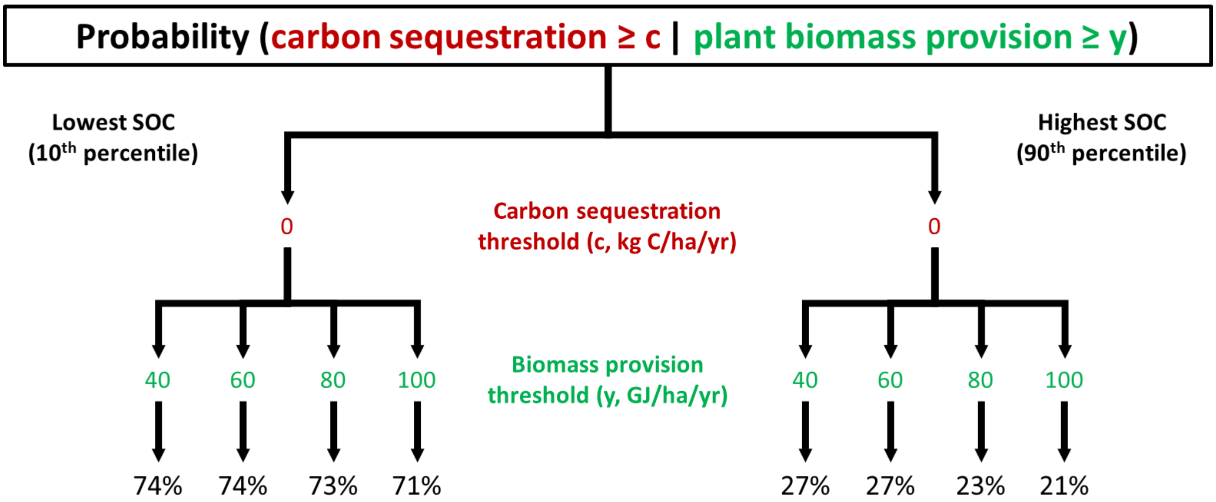

Figure 8. A decision tree of conditional probabilities of carbon sequestration (CS) exceeding a given threshold 'c' (kg C ha^{-1} yr^{-1}) as a function of plant biomass provision (YE) exceeding a given threshold 'y' (GJ ha^{-1} yr^{-1}) from extrapolation of STICS predictions for sites with the lowest or highest soil organic carbon (SOC) contents. For reference, mean yields of maize grain (7.66 t DM ha^{-1}) and wheat (6.48 t DM ha^{-1}) in the study area would provide a mean of 96.8 GJ ha^{-1} yr^{-1} over the 2-year rotation.

Trade-offs may need to be made between the threshold of a regulating SES (GW or CS) and the certainty that it can be achieved: more certainty that a lower threshold can be achieved or, conversely, less certainty that a higher threshold can be achieved. The influence of weather conditions and soil properties must also be considered when estimating probabilities that alternative options can achieve target levels of SES.

4.2. The utility of vine copulas compared to those of other statistical methods

Using the same dataset, Ellili-Bargaoui et al. (2021) developed a correlation network chart to visualize relationships among the mean annual provision of YE, GW and CS and other SESs for all 64 sites over the 31-year simulation (Figure A5). It illustrated a strong negative correlation between YE and GW (Pearson correlation coefficient $r = -0.86$) and no significant correlation between YE and CS ($r = 0.13$). When considering soil properties (e.g., SOC content), the correlation network chart illustrated that SOC had a significantly negative correlation with YE ($r = -0.45$) and CS ($r = -0.66$) but no significant correlation with GW ($r = 0.16$). While Ellili-Bargaoui et al. (2021) used PCA to identify relations among groups of SES, our use of vine copulas specifically enabled us to model degrees of dependence among SESs, such as simple dependence between two SESs and more complex dependence among three or more SESs. In addition, copula models can be used to extrapolate the original sample to a larger one by combining it with the MC method, unlike the correlation network chart and PCA. Copulas enable one to model dependence, if it exists, between the highest or lowest values of pairs of variables (Embrechts et al., 2002). Variables that have non-normal distributions and the potential to have threshold effects on other variables at unusually high or low values (i.e., tail dependence) are particularly suited for analysis by the copula method.

4.3. Limitations and perspectives of the study

The representativeness of this study's results required assuming that STICS accurately predicted the SESs studied. Because biophysical indicators of SESs are often difficult to measure, soil processes are usually simulated to estimate them based on weather data and soil properties. The lack of tail dependence for either pair of SESs studied and the weak correlation between YE and CS or GW limited the added value of the copula method. The study could be extended to investigate the dependence structure among additional SESs studied by Ellili-Bargaoui et al. (2021) (e.g., water-to-plant provision, water quality regulation, N-to-plant provision) as a function of other soil properties (e.g., pH and clay contents of the topsoil, maximum rooting depth), after first identifying significant and strong correlations among these variables to avoid redundant information. Furthermore, the probability of two SESs simultaneously exceeding respective thresholds, and not only one SES doing so, as in the present study, can be investigated given another SES exceeding a given threshold. We did not analyze these probabilities, since the relationships of the two regulating SES as a function of the provisioning SES best fit an independence copula. In addition, dynamic dependence among SESs could also be studied by applying copula modeling to time series of SESs.

5. Conclusion

We investigated how dependence between regulating and provisioning SESs can vary as a function of their ranges of variation by applying vine copula models as a function of a weather condition (i.e., ER) or soil property (i.e., SOC content in the topsoil). Although correlation coefficients can quantify the strength and direction of linear relationships between SESs, they are too simple to describe the complexity of this dependence. The vine copula models used enabled us to formalize the dependence structure, if it existed, among the SESs studied and then to extrapolate their joint variation from the original samples using the MC method. This approach estimated the potential to achieve certain target levels of regulating SESs – groundwater recharge and C sequestration – as a function of variations in a provisioning SES – plant biomass provision. We found that contrasting weather conditions and a soil property could influence the potential to improve one SES as a function of another SES. More complex dependence among a bundle of ESs (i.e., four or more) could be studied using appropriate multivariate copula models. Dynamic relationships among SESs could also be studied by applying copula modeling to time series of SESs.

Conflict of interest statement

This manuscript has not been published and is not under consideration by another journal. The authors have approved the manuscript and agree with submission to your esteemed journal. There are no conflicts of interest to declare.

Data availability statement

Data sharing is not applicable to this article since no new data were created in this study.

Authorship contribution statement

Tristan Senga Kiessé: Conceptualization; formal analysis; methodology; visualization; writing – original draft. Blandine Lemercier: Conceptualization; data curation; funding acquisition; methodology; writing – review and editing. Michael S. Corson: Conceptualization; methodology; visualization; writing – review and editing. Yosra Ellili-Bargaoui:

Conceptualization; data curation; funding acquisition; methodology; writing – review and editing. Jihad Afassi: formal analysis; methodology. Christian Walter: Conceptualization; data curation; funding acquisition; methodology; writing – review and editing.

Acknowledgments

We thank the INRAE division "Agronomy and environmental sciences for agroecosystems" (AgroEcoSystem) for its financial support. This research was also developed in the framework of the European Joint Program for SOIL "Towards climate smart sustainable management of agricultural soils" (EJP SOIL), funded by the European Union Horizon 2020 research and innovation programme (Grant Agreement N 862695).

References

Aas, K., Czado, C., Frigessi, A., Bakken, H., 2009. Pair-copula constructions of multiple dependence. Insurance: Mathematics and economics 44, 182-198.
Agreste, 2021. Statistique agricole annuelle. Cultures développées (hors fourrage, prairies, fruits, fleurs et vigne). Ministère de l'agriculture, https://agreste.agriculture.gouv.fr/agreste-web/disaron/SAANR_DEVELOPPE_2/detail/.
Arrouays, D., Grundy, M.G., Hartemink, A.E., Hempel, J.W., Heuvelink, G.B., Hong, S.Y., et al., 2014. GlobalSoilMap: Toward a fine-resolution global grid of soil properties. Advances in agronomy 125, 93-134.
Bretagne Environnement, 2020. https://bretagne-environnement.fr/donnees-bilan-climatique-bretagne.
Brisson, N., Launay, M., Mary, B., Beaudoin, N., 2009. Conceptual basis, formalisations and parameterization of the STICS crop model. Editions Quae.
Brisson, N., Ruget, F., Gate, P., Lorgeou, J., Nicoullaud, B., Tayot, X., et al., 2002. STICS: a generic model for simulating crops and their water and nitrogen balances. II. Model validation for wheat and maize. Agronomie 22, 69-92.
Calzolari, C., Ungaro, F., Filippi, N., Guermandi, M., Malucelli, F., Marchi, N., et al., 2016. A methodological framework to assess the multiple contributions of soils to ecosystem services delivery at regional scale. Geoderma 261, 190-203.
Ching, J., Phoon, K.-K., Chen, C.-H., 2014. Modeling piezocone cone penetration (CPTU) parameters of clays as a multivariate normal distribution. Canadian Geotechnical Journal 51, 77-91.
Churchman, G.J., Singh, M., Schapel, A., Sarkar, B., Bolan, N., 2020. Clay minerals as the key to the sequestration of carbon in soils. Clays and Clay Minerals 68, 135-143.
Coles, S., Heffernan, J., Tawn, J., 1999. Dependence measures for extreme value analyses. Extremes 24, 339-365.
Cong, R., Brady, M., 2012. The interdependence between rainfall and temperature: copula analyses. Sci World J 2012: 1–11.
Constantin, J., Beaudoin, N., Launay, M., Duval, J., Mary, B., 2012. Long-term nitrogen dynamics in various catch crop scenarios: test and simulations with STICS model in a temperate climate. Agriculture, Ecosystems & Environment 147, 36-46.
Constantin, J., Le Bas, C., Justes, E., 2015. Large-scale assessment of optimal emergence and destruction dates for cover crops to reduce nitrate leaching in temperate conditions using the STICS soil–crop model. European Journal of Agronomy 69, 75-87.

Coucheney, E., Buis, S., Launay, M., Constantin, J., Mary, B., de Cortázar-Atauri, I.G., et al., 2015. Accuracy, robustness and behavior of the STICS soil–crop model for plant, water and nitrogen outputs: evaluation over a wide range of agro-environmental conditions in France. Environmental Modelling & Software 64, 177-190.
Czado, C., Nagler, T., 2022. Vine copula based modeling. Annual Review of Statistics and Its Application 9, 453-477.
Demestihas, C., Plénet, D., Génard, M., de Cortazar-Atauri, I.G., Launay, M., Ripoche, D., et al., 2018. Analyzing ecosystem services in apple orchards using the STICS model. European Journal of Agronomy 94, 108-119.
Dominati, E., Mackay, A., Lynch, B., Heath, N., Millner, I., 2014. An ecosystem services approach to the quantification of shallow mass movement erosion and the value of soil conservation practices. Ecosystem Services 9, 204-215.
EC, 1991. Council Directive 91/676/EEC of 12 December 1991 concerning the protection of waters against pollution caused by nitrates from agricultural sources. Official Journal of the European Union 375, 1-8.
Egoh, B., Reyers, B., Rouget, M., Richardson, D.M., Le Maitre, D.C., van Jaarsveld, A.S., 2008. Mapping ecosystem services for planning and management. Agriculture, Ecosystems & Environment 127, 135-140.
Ellili-Bargaoui, Y., Walter, C., Lemercier, B., Michot, D., 2021. Assessment of six soil ecosystem services by coupling simulation modelling and field measurement of soil properties. Ecological Indicators 121, 107211.
Embrechts, P., Mcneil, A., Straumann, D., 2002. Correlation and dependence in risk management: properties and pitfalls. Risk Management: Value at Risk and Beyond. Cambridge University Press, pp. 176--223.
FAO, 2001. Food balance sheets. A handbook. Food and Agricultural Organization of the United Nations, Rome, p. 95.
Grace, J.B., 2006. Structural equation modeling and natural systems. Cambridge University Press.
Joe, H., 1993. Parametric families of multivariate distributions with given margins. Journal of Multivariate Analysis 46, 262-282.
Joly, F., Benoit, M., Martin, R., Dumont, B., 2021. Biological operability, a new concept based on ergonomics to assess the pertinence of ecosystem services optimization practices. Ecosystem Services 50, 101320.
Lee, H., Lautenbach, S., 2016. A quantitative review of relationships between ecosystem services. Ecological Indicators 66, 340-351.
Lemke, R., VandenBygaart, A., Campbell, C., Lafond, G., Grant, B., 2010. Crop residue removal and fertilizer N: effects on soil organic carbon in a long-term crop rotation experiment on a Udic Boroll. Agriculture, Ecosystems & Environment 135, 42-51.
Leong, R.A.T., Fung, T.K., Sachidhanandam, U., Drillet, Z., Edwards, P.J., Richards, D.R., 2020. Use of structural equation modeling to explore influences on perceptions of ecosystem services and disservices attributed to birds in Singapore. Ecosystem Services 46, 101211.
Levavasseur, F., Mary, B., Christensen, B.T., Duparque, A., Ferchaud, F., Kätterer, T., et al., 2020. The simple AMG model accurately simulates organic carbon storage in soils after repeated application of exogenous organic matter. Nutrient Cycling in Agroecosystems 117, 215-229.
Li, D.-Q., Jiang, S.-H., Wu, S.-B., Zhou, C.-B., Zhang, L.-M., 2013. Modeling multivariate distributions using Monte Carlo simulation for structural reliability analysis with complex performance function. Proceedings of the Institution of Mechanical Engineers, Part O: Journal of Risk and Reliability 227, 109-118.

Lü, T.-J., Tang, X.-S., Li, D.-Q., Qi, X.-H., 2020. Modeling multivariate distribution of multiple soil parameters using vine copula model. Computers and Geotechnics 118, 103340.
Mouchet, M.A., Lamarque, P., Martín-López, B., Crouzat, E., Gos, P., Byczek, C., Lavorel, S., 2014. An interdisciplinary methodological guide for quantifying associations between ecosystem services. Global Environmental Change 28, 298-308.
Nadarajah, S., Afuecheta, E., Chan, S., 2018. A compendium of copulas. Statistica 77, 279–328.
Nagler, T., 2014. Kernel methods for vine copula estimation. Department of Mathematics. Technische Universität München.
Nelson, E., Mendoza, G., Regetz, J., Polasky, S., Tallis, H., Cameron, D., et al., 2009. Modeling multiple ecosystem services, biodiversity conservation, commodity production, and tradeoffs at landscape scales. Frontiers in Ecology and the Environment 7, 4-11.
OJFR, 2011. Arrêté du 19 décembre 2011 relatif au programme d'actions national à mettre en œuvre dans les zones vulnérables afin de réduire la pollution des eaux par les nitrates d'origine agricole. https://www.legifrance.gouv.fr/jorf/id/JORFTEXT000025001662.
Olson, K.R., Al-Kaisi, M., Lal, R., Morton, L.W., 2017. Soil ecosystem services and intensified cropping systems. Journal of Soil and Water Conservation 72, 64A-69A.
Paustian, K., 2014. Carbon Sequestration in Soil and Vegetation and Greenhouse Gases Emissions Reduction. In: Freedman, B. (Ed.), Global Environmental Change. Springer Netherlands, Dordrecht, pp. 399-406.
R Core Team, 2020. R: A language and environment for statistical computing. R Foundation for Statistical Computing, Vienna, Austria.
Radcliffe, D., Simunek, J., 2012. Water flow in soils. In: Huang, P., Li, Y., Sumner, M. (Eds.), Handbook of soil sciences: properties and processes. CRC Press Taylor and Francis Group, pp. 5.1-5.34.
Schepsmeier, U., Stoeber, J., Brechmann, E., et al., 2015. VineCopula:Statistical Inference of Vine Copulas. R package version 1.6-1.
Schnebelen, N., Nicoullaud, B., Bourennane, H., Couturier, A., Verbeque, B., Revalier, C., et al., 2004. The STICS model to predict nitrate leaching following agricultural practices. Agronomie 24, 423-435.
Sklar, A., 1959. Fonctions de répartition à n dimensions et leurs marges. Publications de l'Institut de Statistique de l'Université de Paris 8, 229-231.
Thapa, R., Tully, K.L., Cabrera, M.L., Dann, C., Schomberg, H.H., Timlin, D., et al., 2021. Effects of moisture and temperature on C and N mineralization from surface-applied cover crop residues. Biology and Fertility of Soils 57, 485-498.
Wu, J., Jin, X., Feng, Z., Chen, T., Wang, C., Feng, D., Lv, J., 2021. Relationship of Ecosystem Services in the Beijing–Tianjin–Hebei Region Based on the Production Possibility Frontier. Land 10, 881.